An improved model of continuous leaching systems using segregation approach

Abdolrahim Foroutan [a], Hojat Naderi [a, *], Mohammad Reza Khalesi [b], Reza Dehghan [a]

[a] Mining and Metallurgical Engineering Department, Yazd University, Yazd, Iran
[b] Department of Mining Engineering, Tarbiat Modares University, Tehran, Iran

ABSTRACT

In this study, a simplified dissolution model has been developed to evaluate the performance of continuous leaching reactors. The model considers continuous reduction of the surface area of particles using the distribution of their size and residence time. The model was validated by the bioleaching of a pyrite-arsenopyrite concentrate in the pilot plant scale, which resulted in good agreement between the experimental data and the predicted values. The developed model was also used to predict the outlet mass density function of particles, whose results showed that the mean particle size would not necessarily decrease as the mean residence time in the leaching process decreased. Using this model, the effect of operating parameters (e.g., particle size distribution, inlet flow, reagent concentration, kinetic parameters, and the type of residence time distribution) on the reactor performance can be predicted. Therefore, the model can be used for dynamic and static analyses of leaching circuits as well as designing and optimizing the processing plants.

Keywords : Continuous leaching, Dissolution modeling, Particle size, Residence time

1. Introduction

Modeling leaching reactors is among engineering aspects of hydrometallurgical processes that can be used for design and scale-up purposes as well as for optimizing the operating conditions such as feed flow rate, chemical reagents flow rate, temperature, pressure and etc., in order to obtain the highest amount of conversion [1]. A powerful leaching model permits predicting the operation status in a specified reactor with a set of input data such as particle size distribution (PSD), residence time distribution (RTD), and leaching kinetics of the particles.

One of the methodologies used for Modeling multistage leaching reactors is the population balance model (PBM) based on conserving the number of particles, as shown in equation 1 [2-4]:

$$\frac{d[R(l,L)n(l,L)]}{dl} = \frac{1}{\tau}[n_f(l,L) - n(l,L)] \tag{1}$$

where $n(l,L)dldL$ is the number of particles per unit volume in size range of l to $l+dl$ which has an initial size range of L to $L+dL$. The symbol τ is the mean residence time distribution (mRTD) and $R(l,L)$ is the rate of particle shrinkage obtained from the unreacted shrinkage-core model.

The segregated flow model (SFM) is another method that assumes each particle behaves as a tiny batch reactor that remains in contact with bulk solution during its residence in the reactor [5, 6]. The amount of conversion for a steady-state reactor is given as equation 2:

$$1 - X_B = \int_0^\infty \int_0^\infty [1 - X_B(l,t)]f(l)E(t)dldt \tag{2}$$

where X_B is the batch conversion, $f(l)$ is the mass density function of particles in the inlet stream and $E(t)$ is the exit age distribution of the reactor.

As equations (1) and (2) show, the PBM approach applies mRTD, while SFM can use any type of experimental or ideal RTD. Dixon [7] mentioned that PBM is a rough and problematic method for Modeling the leaching reactors because of its tendency towards infinitude as particle size moves toward zero. Thus, SFM and its improved model 'Multiple Convolution Integral (MCI)' have remarkable potential for modeling and simulating leaching reactors.

Kotsiopoulos [8] applied a segregation approach to the population balance model of a continuous bioleaching system that can be used for dynamic systems as well. In this approach, the overall reaction rate (mole/volume/time) and conversion were best described and predicted by incorporating both the mass density function and the internal age distribution. The differential form of the overall reaction rate is shown in Equation 3:

$$r^R = \int_0^\infty \int_0^\infty r'' A^P(\theta,l) \frac{M^P(\theta,l)}{V^R} \varphi_{MS} N^T I(\theta) f(l) d\theta dl \tag{3}$$

where r^R ($\frac{mol}{m^3.s}$) is the overall reaction rate, r'' ($\frac{mol}{m^2.s}$) is the intrinsic surface reaction rate, A^P is the specific particle surface area, M^P is the particle mass, V^R is the reactor volume, ϕ_{MS} is the fraction of pure sulfide mineral in the ore, and N^T is the total number of particles in the reactor. According to equation 4, the total number of particles should appear with the number density function than the mass density function. Hence, equation 3 is not mathematically sensible.

* Corresponding author. E-mail address: naderi@yazd.ac.ir (H. Naderi).

$$\begin{bmatrix} Total\ mass\ of\ particles \end{bmatrix}\begin{bmatrix} Mass\ fraction\ of \\ particles\ of\ size\ L \end{bmatrix} = \begin{bmatrix} Mass\ of\ a \\ particle\ of\ size\ L \end{bmatrix}\begin{bmatrix} Number\ of \\ particles\ of\ size\ L \end{bmatrix} \qquad M_0 f(L)d(L) = M^P N^T f_n(L)d(L) \qquad (4)$$

where M_0 (kg) is the total mass of particles inside the reactor, $f_n(L)d(L)$ is the number fraction of particles with size L to $L+dL$, $f(L)d(L)$ is the mass fraction of particles with size L to $L+dL$ and M^P (kg) is the mass of a particle [4].

The purpose of this study is to develop an overall reaction rate model for continuous leaching systems that use both segregation flow and population balance concepts. Here, the correct relationship between number and mass density functions of particles was used to extend a simpler model than equation 3 that uses the total number of particles in the mass density function at one side of the equation. The outlet mass density function of particles was also derived from the developed model. Using the outlet mass density function of particles, the performance of subsequent tanks can be evaluated. The presented models can be used for sensitivity analysis of system factors for improving the design, control and performance of metallurgical plants.

2. Model development

2.1. Overall reaction rate

In leaching reactor Modeling, it is necessary to obtain the equation for the overall reaction rate, designing, and circuit analysis of the leaching process. The overall reaction rate of sulfide minerals is usually described based on the mineral's surface oxidation rate [9-11]. Hence, particles of different sizes will show different rates of leaching; therefore, in continuous systems, PSD affects the overall reaction rate and should be considered for Modeling purposes. Besides, the reaction between the particles and reactants does not take place at the same time, meaning that RTD can be considered for the system. Consequently, the overall reaction rate should be described by integrating the PSD of the inlet stream, the shrinkage kinetic of particles, and the RTD of particles inside the reactor. Mckiben [10] showed that for the batch system, the overall reaction rate can be described based on equation 5:

$$r^R = r_{sp}\frac{A}{V} \qquad (5)$$

where r_{sp} is the specific rate law ($\frac{mol}{m^2.s}$), A is the total surface area of particles (m^2), and V is the batch reactor volume (m^3). The surface area of one particle and hence its diameter decreases due to the reaction, which depends on its age in the reactor. The dependency of particle diameter to the shrinking particle kinetic and time has been described as equation 6 [9, 8]:

$$l_{(\theta,L)} = L - (\frac{2r_{sp}}{\rho}M_{MeS}).\theta \qquad (6)$$

where $l_{(\theta,L)}$ is the diameter of the particle (m) with age θ with the initial size of L, ρ is the particle density ($\frac{kg}{m^3}$), and M_{MeS} is the molar mass of the sulfide mineral ($\frac{kg}{mol}$). For continuous systems, the total surface area, $A_{(\theta,L)}$, is obtained by summing the surface area of all particles in the reactor. On the other hand, the number of particles in each size fraction is not the same and the feed has its density function based on the number of particles. Hence, for the total surface area, $A_{(\theta,L)}$, with age θ, which has the initial diameter of L, equation 7 can be written as follows:

$$A_{(\theta,L)} = \iint a^p_{(\theta,L)} N^T f_n(L)dL\ I(\theta)d\theta \qquad (7)$$

where $a^p_{(\theta,L)}$ is the surface area of the particle with age θ with the initial diameter of L and $I(\theta)$ is the internal age distribution.

Then, if equations 6, 7, and 4 are replaced in equation 5, the overall reaction rate for the continuous system is obtained as follows:

$$r^R = \int_0^\infty\int_0^\infty r_{sp}\frac{M_0}{V}\frac{a^p_{(\theta,L)}}{M^P}f(L)dL\ I(\theta)d\theta = \int_0^\infty\int_0^\infty 6r_{sp}\frac{M_0}{\rho V}\frac{l^2_{(\theta,L)}}{L^3}f(L)dL\ I(\theta)d\theta \qquad (8)$$

where r_{sp} depends on the concentration of the chemical reagent in the pulp and can be explained as $r_{sp} = k\left[C_i\right]^n$, in which k is a constant and C_i is the concentration of reagent i [12]. Therefore, if the parameter N^T is used, the number density function is a suitable function to describe the surface area and equation 3 can be improved to equation 8. In order to simulate the mass density function, Rosin-Rammler's function can be used as equation 9 [13]:

$$f(L) = \frac{m(L/L^*)^{m-1}e^{-(L/L^*)^m}}{L^*} \qquad (9)$$

where m is the distribution parameter, L^* is the normalizing size that is (63.21% passing size for this case) and L has the range of $\{0,\infty\}$.

In equation 8, a perfect mixing tank in a series model can be used for estimating the internal age distribution [13]:

$$E(\theta) = \frac{(\theta/\tau)^{M-1}e^{-\theta/\tau}}{\tau(M-1)!} \qquad (10)$$

where τ is obtained by dividing the tank volume by volumetric flow rate of pulp into the tank. The symbol M is the number of tanks in the series.

2.2. Mass balance of components

For determining the comprehensive description of species concentration over time or in the steady state in a given leaching reactor, the equations that describe different reaction steps need to be combined and integrated into a dynamic mass balance. The mass balance equation can be written in a simplified form as follows [14]:

$$\frac{dC_j}{dt} = \frac{F}{V}(C_{j,feed} - C_j) + \sum_i v_{j,i}r_i^R \qquad (11)$$

where $[C_j]$ is the concentration of species j ($\frac{mol}{m^3}$), F is the volumetric flow rate ($\frac{m^3}{h}$), V is the reactor volume (m^3), $v_{j,i}$ refers to the stoichiometric coefficients that is the number of moles of each species j consumed or produced in reaction i, and r_i^R is the reaction rate of species j in the reaction i.

In population balance modeling, the number density function is balanced directly, but in equation 11, when balancing is carried out on the solid phase, the number of particles and its distribution is embedded in the overall reaction rate (r^R). Therefore equation 11 is also a population balance model due to including PSD that contains both mRTD ($\frac{V}{F}$) and RTD.

2.3. Mass density function of particles in outlet stream

According to equation 6, the diameter of particles decreases over time, hence the PSD of outlet stream should be reconstructed and used for the subsequent tank. Therefore, in order to develop the mass density function of particles, equation 12 is taken into account for the outlet stream as follows:

$$M_{out}f_{out}(L)d(L) = M^P_{out} N^T f_n(L)d(L) \qquad (12)$$

where M_{out} is the total solid flow rate of the outlet, $f_{out}(L)$ is the mass density function of the outlet and M_{out}^p is the mass flow rate of the particle at the outlet that depends on the age and initial size.

Also, the same equation could be written for the inlet stream as equation 13:

$$M_{in} f(L) d(L) = M_{in}^p N^T f_n(L) d(L) \tag{13}$$

where M_{in} is the total mass flow rate in the reactor inlet and M_{in}^p is the mass flow rate of the particle at the reactor inlet.

The comparison of equations 12 and 13 shows that the mass of particles in L to L+dL size fraction decreases. Also, the number of particles is equal to that of the inlet stream, unless the particles disappear due to leaching.

Since the mass of a particle in the outlet depends on the initial size and age of particles inside the reactor, equation 14 can be written for outlet stream using equation 12 and 13:

$$f_{out}(L) = \frac{M_{in}}{M_{out}} \int_{\theta=0}^{\theta=\infty} \frac{M_{out}^p}{M_{in}^p} f(L) d(L) I(\theta) d\theta \tag{14}$$

If equation 14 is simplified, equation 15 can be written:

$$f_{out}(L) = \frac{1}{1-X} \int_{\theta=0}^{\theta=\infty} (1 - \frac{2 r_{sp} M_{MeS}}{\rho L} \theta)^3 f(L) d(L) I(\theta) d\theta \tag{15}$$

Equation 15 can be solved directly or by variable transformation presented by Dixon [5].
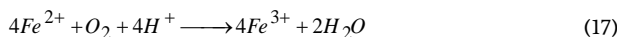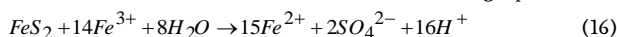
3. Validation and simulation

For validating the developed model, the bioleaching data of a gold bearing concentrate from the pyrite-arsenopyrite flotation process of Fairview Mine near Barberton, Transvaal, South Africa, were used [15]. The size and chemical analysis of the feed is shown in Table 1.

Table 1. Analysis of the Fairview concentrate used as the validation dataset [15] .

Chemical analysis		Size analysis	
Component	Analysis%	Size (μm)	Mass retained%
Total Sulphur	23.2	+71	4-6
[Iron	24.7	+56	8-11
Arsenic	5.5	+48	4-5
Gold (g/t)	143.6	+36	5-6
		+28	10-11
		+20	7-8
		-20	50-60

The volume of the first parallel tanks was 10 m³. Temperature and pH in the plant were maintained at $40\,^{\circ}\text{C}$ and 1.6, respectively. The modified version of the 9K nutrient medium was used initially. The used culture was a mixed *Thiobacillus* culture that had become very well-adopted to the Fairview concentrate. The plant feed was maintained at a pulp density of 120 kg m^{-3}, equivalent to a liquid-to-solid ratio of 8:1. When the plant was running appropriately and the operation factors were adjusted at the mentioned amounts, the flow rate of slurry was regulated to obtain the desired residence time. Once the operation at a specific residence time was stabilized, the feed rate was increased to evaluate the new steady-state condition [15].

The leaching of pyrite concentrate with ferric ion and bacterial oxidation of ferrous ion can be described as the following equations:

$$FeS_2 + 14Fe^{3+} + 8H_2O \rightarrow 15Fe^{2+} + 2SO_4^{2-} + 16H^+ \tag{16}$$

$$4Fe^{2+} + O_2 + 4H^+ \longrightarrow 4Fe^{3+} + 2H_2O \tag{17}$$

The mass balance equation for pyrite can be written as equation 18:

$$\frac{d[FeS_2]}{dt} = \frac{[Fes_2]_{in} - [Fes_2]}{\tau} - r^R \tag{18}$$

The amount of conversion in the steady-state is obtained according to equation 18:

$$X = \frac{r^R \tau}{[FeS_2]_{in}} \tag{19}$$

The results of applying equation 19 to the experimental data is shown in Fig. 1. According to [14], the order of reaction for the sulfide mineral is usually 0.5 and in this research, the order of reaction, n, and the constant of specific rate law, k, was obtained 0.55 and 2.63×10^{-3} $\frac{mol^{0.45}}{m^{1.35} \, day}$, respectively. In this section, the ideal RTD with one tank was used to optimize k and n. If the experimental RTD with non-ideal characteristics, such as dead volume or by pass flow rate [16, 17], are available for the system, more accurate values can be obtained for optimization purposes. In order to evaluate the effect of RTD and PSD, the new distribution of these functions should be used for optimizing and obtaining the new amounts for n and k. When the parameters n and k are available, the equation (11) can be used for calculating the concentration of other elements using the related reaction rates. In this study, all of the calculations and plots were carried out using the MATLAB package.
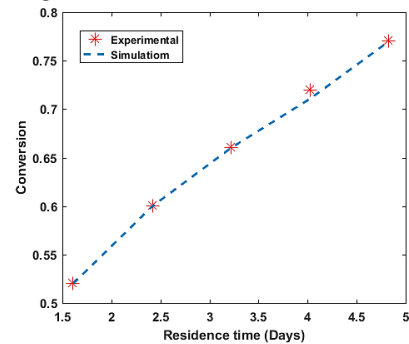

Fig. 1. Fitting the model to the experimental data of the first tanks.

The result of fitting the model on the overall reaction rate is shown in Fig. 2. As shown, the overall values of reaction rate modeling containing RTD and PSD are in good agreement with the experimental data. When the mean residence time is increased, the time required for dissolution increases and some of the particles disappear. Hence the number of particles decreases and due to direct relation of the overall reaction rate to the available surface area, the overall reaction rate decreases. Therefore, for improving the performance of the reactor, effective factors on the overall reaction rate, such as mass transfer of oxygen and the ferric to ferrous ratio, can be included. Enhancing the mentioned factors improves the overall reaction rate. The shape of the mass density function can affect the overall reaction rate, and the larger distribution parameter, L^*, with the same mean particle size, can lead to a positive result for the overall reaction rate.
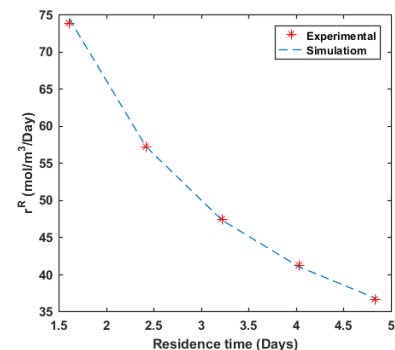

Fig. 2. Fitting the overall reaction rate to the experimental data.

Regarding decreasing the particle size due to the leaching mechanism, Dixon [7] presented equation 20 as a new method to predict the mass density function of particles in the outlet stream of reactor N, normalized to the distribution of feed, $f(\xi)$, using the unreacted fraction in the tank $1-X$. The area under the actual mass density function or its normalized distribution at the outlet of any reactor should independently be 1, while according to the MCI method, this area decreases similar to the fraction unreacted in the tanks (Fig. 3). On the other hand, the MCI method, which is not a new method, is a different solution to the SFM method.

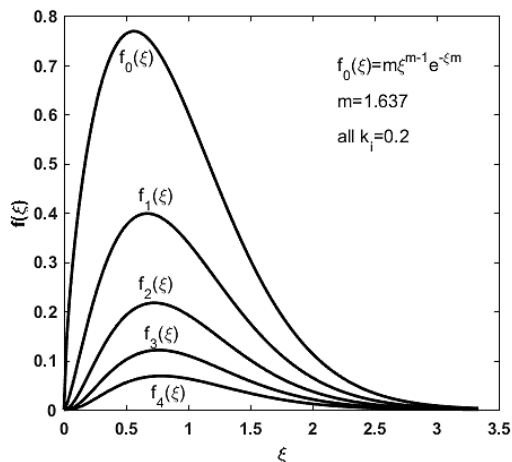$$1-\bar{X}_N = \int_0^{\xi_{max}} f_N(\xi)d\xi \tag{20}$$

Fig. 3. Reconstructed PSD of the outlet stream of reactor N [5].

The simulation result of the outlet mass density function for different mean residence times is shown in Fig. 4.
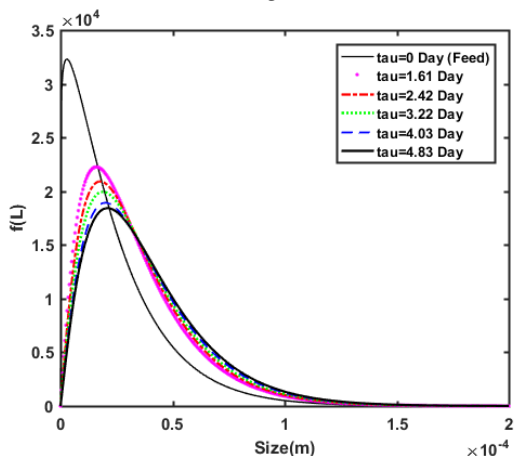

Fig. 4. The simulation result of the particle mass density function for the outlet stream for different mean residence times.

As Fig. 4 shows, the fraction of particles in smaller sizes decreases with increasing the mean residence time. On the other side, the mean particle size is not necessarily decreased. The reason for this can be due to the complete leaching and disappearance of a huge number of particles in the ultrafine size fraction that shifts the mean particle size toward the size of larger particles. According to [18], this phenomenon is probably related to the distribution of feed material that increases or decreases the mean particle size of the outlet stream compared to the inlet flow. Despite their rather narrow size distribution, the particles leaving the reactor are, on average, smaller than those entering it. However, for the wide distribution, the mean particle size is larger (Figs. 5, 6).
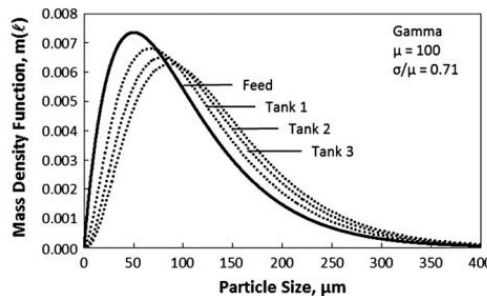

Fig. 5. The mass density function of particles leaving equally-sized reactors with a wide distribution of feed particles [18].
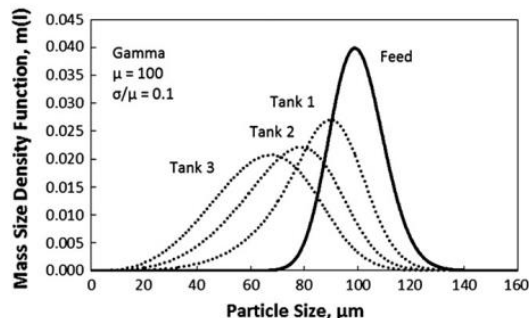

Fig. 6. The mass density function of particles leaving equally-sized reactors with a narrow distribution of feed particles [18].

In Fig. 5 (and 6), the mass density of particles in the outlet stream was calculated by the population balance model, which was in agreement with the results of equation (15) in Fig. 4.

The same result has been reported by [19] for the mass density function of chalcopyrite leaching in each autoclave compartment. Similarly, the reconstructed PSD of the outlet stream proposed for Fig. 3 is shown in Fig. 7. The same trend can also be seen for this example.
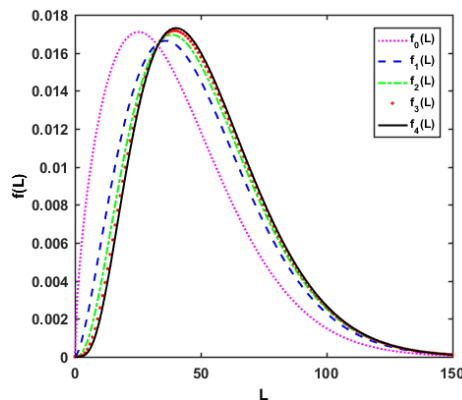

Fig. 7. The mass density function for the outlet stream of the reactors proposed for Fig. 3.

4. Conclusion

The overall reaction rate, which considers the mass density function and the internal age distribution, was developed and validated for pilot plant data. The results showed a good agreement between the experimental data and the Modeling values. Despite the models that are used only for estimating the amount of conversion for steady-state systems, modeling the overall reaction rate can be used in dynamic systems. The improved model can be also used for predicting the mass density function of the outlet stream. The model showed that the mean particle size of the reactor outlet depends on the feed PSD and kinetics of leaching, and can be larger than the feed due to the disappearance of ultrafine particles.

REFERENCES

[1] Papangelakis, V. & Demopoulos, G. (1993). Modeling, Simulation and Control of Hydrometallurgical Processes: Proceeding of the international symposium on Modeling, simulation and control of hydrometallurgical processes, Quebec City. Quebec, August 24-September2.

[2] Coelho, F.E.B., Balarini, J. C., Araújo, E.M.R., Miranda, T.L.S., Peres, A. E. C., Martins A.H., & Salum, A. (2018). Roasted zinc concentrate leaching: Population balance modeling and validation. *Hydrometallurgy*, 175(0), 208-217. doi: https://doi.org/10.1016/j.hydromet.2017.11.013

[3] Crundwell, F. & Bryson, A. (1992). The Modeling of particulate leaching reactors-the population balance approach. *Hydrometallurgy*, 29(1-3), 275-295. doi: https://doi.org/10.1016/0304-386X(92)90018-U

[4] Sohn, H.Y. & Wadsworth, M.E. (2013). Rate processes of extractive metallurgy. *Springer Science & Business Media*. doi: https://doi.org/10.1007/978-1-4684-9117-3

[5] Dixon, D.G. (1995). Improved methods for the design of multistage leaching systems. *Hydrometallurgy*, 39(1), 337-351. doi: https://doi.org/10.1016/0304-386X(95)00040-N

[6] Peters, E. (1991). The mathematical modeling of leaching systems. *JOM*, 43(2), 20-26.

[7] Dixon, D.G. (1996). The multiple convolution integral: a new method for modeling multistage continuous leaching reactors. *Chemical engineering science*, 51(21), 4759-4767. doi: https://doi.org/10.1016/0009-2509(96)00334-X

[8] Kotsiopoulos, A., Hansford, G.S., & Rawatlal, R. (2008). An approach of segregation in modeling continuous flow tank bioleach systems. *AIChE journal*, 54(6), 1592-1599. doi: https://doi.org/10.1002/aic.11479

[9] Drossou, M. (1986). The kinetics of the bioleaching of a refractory gold-bearing pyrite concentrate. University of Cape Town. doi: https://open.uct.ac.za/bitstream/handle/11427/23206/Drossou_kinetics_1982.pdf?sequence=1

[10] McKibben, M.A. & Barnes, H.L. (1986). Oxidation of pyrite in low temperature acidic solutions: Rate laws and surface textures. *Geochimica et Cosmochimica Acta*, 50(7),1509-1520. doi: https://doi.org/10.1016/0016-7037(86)90325-X

[11] Wiersma, C. & Rimstidt, J. (1984). Rates of reaction of pyrite and marcasite with ferric iron at pH 2. *Geochimica et Cosmochimica Acta*, 48(1), 85-92. doi: https://doi.org/10.1016/0016-7037(84)90351-X

[12] Boon, M.(1996). Theoretical and experimental methods in the Modeling of bio-oxidation kinetics of sulphide minerals. TU Delft, Delft University of Technology. doi: http://resolver.tudelft.nl/uuid:d97e28be-eb6d-452b-8648-807c192a2600

[13] Vignes, A. (2013). Extractive metallurgy 3: Processing operations and routes. *John Wiley & Sons*. doi: 10.1002/9781118617106

[14] Petersen, J.(2010). Modeling of bioleach processes: connection between science and engineering. *Hydrometallurgy*, 104(3-4), 404-409. doi: https://doi.org/10.1016/j.hydromet.2010.02.023

[15] Hansford, G. & Miller, D.(1993). Biooxidation of a gold-bearing pyrite-arsenopyrite concentrate. *FEMS microbiology reviews*.,11(1-3), 175-181.

[16] de Andrade Lima, L. & Hodouin, D. (2005). Residence time distribution of an industrial mechanically agitated cyanidation tank. *Minerals engineering*, 18(6), 613-621. doi: https://doi.org/10.1016/j.mineng.2004.10.006

[17] Murphy, T. (2002). Residence Time Distribution of Solid Particles in a CSTR. McGill University Libraries. doi: http://digitool.Library.McGill.CA:80/R/-?func=dbin-jump-full&object_id=79251&silo_library=GEN01

[18] Crundwell, F., Preez, N, Du. & Lloyd, J. (2013). Dynamics of particle-size distributions in continuous leaching reactors and autoclaves. *Hydrometallurgy*, 133, 44-50. doi: https://doi.org/10.1016/j.hydromet.2012.11.016

[19] Saloojee, F. & Crundwell, F, K. (2016). Optimization of circuits for pressure leaching of sulphide ores and concentrates. *Journal of the Southern African Institute of Mining and Metallurgy*, 116(6), 517-524. doi: 10.17159/2411-9717/2016/v116n6a5.